# Dual Optomechanical Cavities for All-Optical Actuation and Sensing of Mechanical Motion

Xia Ji, Xiong Shuidong, Cao Chunyan, Wang Jianfei, and Wu Yanqun

***Abstract*—Cavity optomechanics in the photonic devices enables a light-matter interaction in the chip-scale systems via the optical force driven mechanical motion. In this paper, a pump-probe scheme consisting of dual optomechanical cavities is proposed for the first time, where one optical cavity driven by a high input power act as a pump channel and the other one is used as a probe channel to detect the dynamical motion of mechanical resonator. Moreover, modulation of the optical force in the pump channel is achieved to observe the amplification of mechanical motions. As the light input of the pump channel increases, the dynamical displacement of the mechanical resonator is theoretically actuated to 4.8 nm$/\sqrt{\text{Hz}}$ at the pump power of 0.75 mW. This all-optical amplification of mechanical motion based on the pump-probe scheme potentially paves the way for the development of optomechanical actuation and switch for the photonic integrated circuits.**

***Index Terms*—Cavity optomechanics, motion amplitude, optical force, photonic crystal cavities.**

## I. Introduction

IN THE recent two decades, the topic of cavity optomechanics (COM) has evolved significantly, with fields focusing on the interplay between optical and mechanical degrees of freedom mediated by the optical force [1]. COM systems have been utilized in detection metrology to produce high-precision measurements for optical detection of displacement [2], mass [3], force [4], acceleration [5], and other parameters. The resonant amplification of both mechanical and optical responses in the COM systems has enabled precision sensing. COM sensors have a small size, low mass, and low power consumption, as well as on-chip integration characteristics, fiber coupling compatibility, and so on [6]. Optomechanical interaction can also be used to investigate the effects of optical force. One optical pump signal can impart sufficient optical force to mechanically displace or deform the optical channel in nanoscale photonic devices, while another probe optical signal takes and alters its propagation. Optomechanical devices with coherent switching can be used as non-volatile memory with nanoscale dimensions, enabling for large-scale integration, high-speed operation, and low power consumption [7]. Cavity optomechanics has a wide range of potential applications, including tunable photonic filters [14] and wavelength routers [8], wavelength conversion [9] and switching [10], and radio-frequency optomechanical oscillators [11].

In the COM systems, this optical force is used to drive the movement or deformation of cavity structures to modify the optical channel and optical signal transmission [12]. This optical force may interact with mechanical resonators in COM systems through strong optomechanical interaction, and it can be achieved in an integrated photonic platform utilizing only one kind of optical material (e.g., silicon and glass) without employing additional electro-optical effects [13]. Due to its resonantly enhanced optomechanical interaction, this optical force is dramatically improved in the high optical quality-factor cavity. The interaction between optical cavities and mechanical resonators has been observed and investigated in order to learn more about those fundamental studies and applications of tunable photonics. In most existing optomechanical systems, however, only a single optical channel is used to launch and detect light coupled into and out of the optical cavity [14]. A fiber taper or integrated waveguide, for example, is evanescently connected with the optical cavity in some COM systems to activate cavity optomechanics and detect dynamical backaction. To detect cavity optomechanics, the pump power should be kept below a threshold to reduce the thermal-optical effect on the optical resonance, however this results in a weak optical force. However, this optical force in the COM system should be sufficient to drive the movement of mechanical parts for all-optical signal conversion. The development of cavity optomechanics and the requirement for substantial optical forces in COM systems using a single coupling channel are at conflict in this scenario. Meanwhile, a single coupling channel is insufficient to transmit both the pump and probe light simultaneously in an optomechanical system when the optical force should be dynamically modulated in order to achieve harmonic amplification of mechanical motion. When both the pump signal and the probe signal are coexisted in the same channel, the frequency-tuned signals are easily coupled with the mechanical resonance signal.

As a result, a hybrid COM system, which consists of two identical optical cavities physically coupled by a mutual mechanical resonator, is an alternative approach to overcome the technical obstacles above. One optical cavity serves as a pump for providing a driving optical force, while the other is employed to detect the mechanical resonator's motion. Two fiber taper coupling channels are also required for launching high optical power into the pump cavity to create the optical force as well

Manuscript received 7 April 2022; revised 25 May 2022; accepted 21 June 2022. Date of publication 27 June 2022; date of current version 7 July 2022. This work was supported by the National Natural Science Foundation of China under Grant 61905283. *(Xia Ji and Xiong Shuidong contributed equally to this work.) (Corresponding author: Cao Chunyan.)*

The authors are with the College of Meteorology and Oceanography, National University of Defense Technology, Changsha 410073, China (e-mail: e0267876@u.nus.edu; nudtxsd@163.com; ccy_nudt@163.com; wangjianfei@163.com; wuyanqun@163.com).

Digital Object Identifier 10.1109/JPHOT.2022.3186408

This work is licensed under a Creative Commons Attribution 4.0 License. For more information, see https://creativecommons.org/licenses/by/4.0/

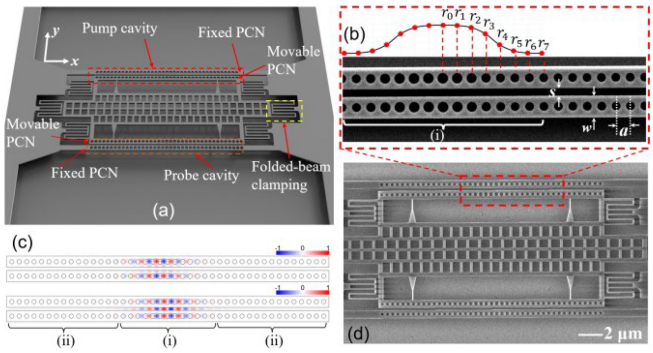


Fig. 1. Configuration of dual optomechanical cavity system. (a) Schematic of dual optomechanical cavities with folded-beam clamping; (b) Geometric size of the coupled PCN cavities; (c) Simulated fundamental resonance modes of the coupled PCN cavities; (d) SEM image of the suspended optomechanical device.

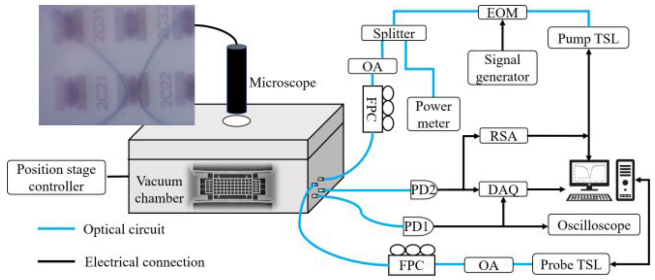


Fig. 2. Experimental measurement setup for charactering dual optomechanical cavities. (EOM: electro-optic modulator, PD = photodetector, TSL: Tunable semiconductor laser, OA: optical attenuator, FPC: Fiber polarization controller, RSA: Real-time signal analyzer, DAQ: Data acquisition device.).

as monitoring the mechanical reaction from the probe cavity. To achieve the harmonic amplification of the mechanical motion in this dual optomechanical system, light launching into the pump cavity should be frequency-tuned. Furthermore, light in these two individual coupling channels can propagate and be detected separately without signal crosstalk.

## II. Dual Optomechanical Cavities for Pump-Probe System

Fig. 1 shows the proposed pump-probe optomechanical system based on the integration of dual optical cavities. As presented in Fig. 1(a), there are two identical silicon coupled photonic crystal nanobeam (PCN) resonators, one serving as the pump cavity and the other acting as the probe cavity. Meanwhile, one PCN resonator is doubly-clamped to the silicon device layer, denoted as fixed PCN, for light launching by contact with a dimpled fiber taper. The other PCN resonator is mechanically anchored with a mechanical element to act as a movable PCN. Here, this mechanical element exploited for the optomechanical interaction serves as a mechanical resonator that is mutually shared by the pump and probe optical cavities, and it is suspended by three pairs of the four folded beams (beam width 120 nm and beam length 2.25 $\mu$m) in a parallel structure, which are employed to achieve a large deflection of the mechanical resonator and avoid the out-of-plane rotation mechanical modes. In each optical cavity, a pair of PCN resonators are coupled to each other and the coupled resonance modes are validated by Lumerical FDTD, as presented in Fig. 1(b) and (c). The single PCN cavity consists of a center defect region (i) and two side mirror regions (ii). Regarding the design steps given in Refs. [15], [16], the design of the proposed PCN starts with determining the sizes of the unit cell, including silicon thickness $t = 220$ nm, width $w = 560$ nm, the maximal and minimal radius of air hole $r_0 = 128$ nm and $r_7 = 106$ nm, and lattice constant $a = 365$ nm. In the defect region, the radii of the remaining seven air holes on each side are tapered by following a symmetric power function to reduce the optical loss (Fig. 1(b)). According to the well-established temporal coupled-mode theory [17], Fig. 1(c) shows the simulated mode profiles of the fundamental even and odd modes under the varying slot gap of 125 nm. It should be noted that there is a peak electric field intensity of $TE_{1,e}$ mode in the center of the slot gap between two nanobeams, which leads to a stronger coupling strength in the slot gap. Therefore, optical resonance at $TE_{1,e}$ mode is preferred to excite a stronger optical force for the actuation. The dual optomechanical system is developed on a silicon-on-insulator (SOI) wafer with a buried-oxide (BOX) layer of 2 $\mu$m thick, as presented in Fig. 1(d). First, the pattern of the dual optomechanical system is defined on the silicon device layer by electron beam lithography (EBL) and a deep reactive ion etching (DRIE) of silicon. Subsequently, the suspended structures are achieved by the removal of the BOX layer by the vapor HF release.

## III. Experimental Results

As shown in Fig. 2, an experimental setup based on two fiber taper-cavity coupling channels is established to demonstrate motion amplification in a low-pressure environment. In the pump light channel, pump laser light from a tunable semiconductor laser (TSL, Santec TSL710, Japan) is modulated by an electro-optical modulator (EOM, MX-LN-0.1-iXblue Photonics, France) to achieve a frequency-tuned light intensity, yielding a frequency-tuned optical force. Subsequently, the modulated light is split into two parts: 99% optical intensity is injected into subsequent optical fiber circuits and 1% intensity is monitored to evaluate light stability and operation wavelength. Subsequently, the 99% optical intensity is reduced through an optical attenuator (OA) and then it is selectively adjusted to excite transverse electric (TE) mode through a fiber polarizer controller (FPC) to ensure efficient optical coupling. Afterward, the TE-polarized light is launched into the pump coupled PCN cavity and the escaped light from the pump cavity is collected back into the same fiber taper. The transmitted optical power from the pump cavity is measured by the high-speed photodetector (PD2, Newport 1802, USA) and is split. To characterize the optical properties of the optomechanical cavity, one group signal is connected with the data acquisition device (DAQ). Synchronization is established between DAQ and pump TSL to obtain the optical transmission spectrum. The other group signal is sent to a real-time signal analyzer (RSA, Agilent N9020A, USA) to measure the power spectral density (PSD) spectrum of the optomechanical system. In the detection of PSD spectra, the wavelength of the laser should be controlled near the optical

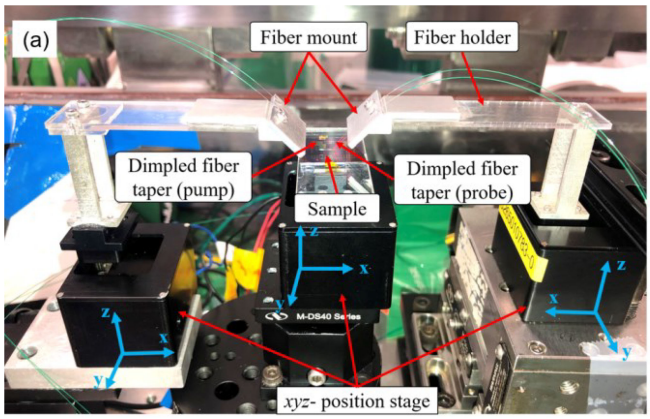


Fig. 3. Alignment of two fiber taper coupling channels and on-chip device.

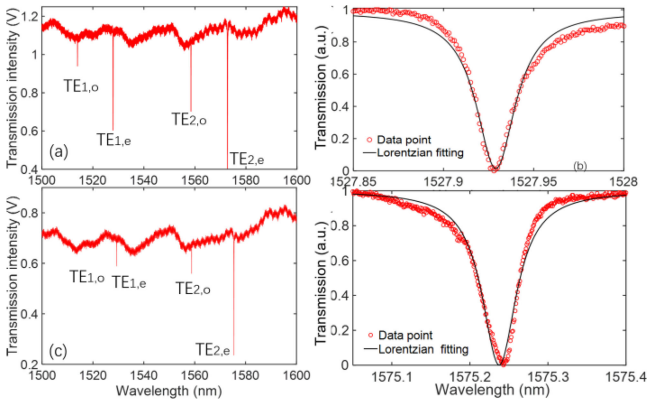


Fig. 4. Optical transmission spectrum of pump and probe optical cavity: (a) Optical resonance of the pump cavity; (b) Normalized $TE_{1,e}$ resonance of the pump cavity with a Lorentzian fitting; (c) Optical resonance of the probe cavity; (d) Normalized $TE_{2,e}$ resonance of the probe cavity with a Lorentzian fitting.

resonance by simultaneously controlling RSA and pump TSL. Both optical and mechanical spectra data are finally processed in the computer. In a similar manner, another tunable laser (TSL, Santec TSL510, Japan) and detection system are added to the probe channel. In addition, an oscilloscope is connected with PD1 in the probe channel to monitor the variation of transmitted light intensity.

In order to observe the cavity optomechanics inside the dual optomechanical cavities, two fiber taper coupling channels are proposed as shown in Fig. 3 to achieve the precise alignment between these pump-probe channels and optomechanical devices. In the two fiber taper channels configuration, two dimpled fiber tapers are employed for the optomechanical measurements for the first time. One dimpled fiber taper is aligned and attached with the fixed PCN of the pump optical cavity, which is known as a pump fiber taper channel. Similarly, the other fiber taper to detect the cavity optomechanics of the probe optical cavity is called a probe fiber taper channel. The precise alignment between the fiber taper and optomechanical device can be finished in the vacuum chamber under microscopic observation. Prior to the experimental measurements, it is significant to give an introduction to the experimental procedure. First, a precise alignment of the pump channel and pump cavity is completed to characterize the optical transmission spectra and mechanical oscillation modes. Similarly, the alignment of the probe channel and probe cavity is finished to check the optical transmission spectra and mechanical oscillation modes. It should be noted that a comparison of the measured results in the pump and probe channels is needed to validate the mechanical oscillation modes and justify the good quality of the suspended mechanical system. Subsequently, characterization of dynamical backactions of cavity optomechanics is conducted in the probe channel. In this case, the pump channel is switched off, so the measured mechanical spectra can exclusively demonstrate a thermal Brownian motion of the mechanical resonator without considering the optical force from the pump channel. Finally, amplification of mechanical motion in the dual optomechanical cavities is observed using the pump-probe channels. Here, the optical power and operation wavelength of the pump channel should be fixed during the monitoring of the mechanical response from the probe channel. Besides, the pump light intensity is modulated around the target mechanical resonant frequency to observe the response of the mechanical resonator and the light intensity in the pump channel is higher than that of the probe channel.

Characterization of this dual optomechanical cavity is conducted under a low-pressure environment ($1 \times 10^{-3}$ mBar). As shown in Fig. 4, the optical resonances of the pump and probe cavities are characterized to determine the operating wavelengths of the pump and probe channels. In the optical transmission spectrum in Fig. 4(a), the first two orders of cavity modes of the pump optical cavity are excited under the input intensity of 80 $\mu$W. Using Lorentzian fitting to calculate the cavity spectrum in Fig. 4(b), the FWHM of the $TE_{1,e}$ cavity mode is solved as 26 pm at the wavelength of 1527.925 nm, which equals an overall $Q_o = 5.9 \times 10^4$. Likewise, optical resonances of the probe optical cavity are also measured as shown in Fig. 4(c) under the input power of 20 $\mu$W. Fig. 4(d) indicates that an FWHM of 53 pm (equivalent to $Q_o = 3.0 \times 10^4$) is obtained via the Lorentzian fitting at the $TE_{2,e}$ resonance of 1575.240 nm. Moreover, optical resonances measured from the pump and probe cavities in Fig. 4 also prove that a good fabrication quality of device is achieved from the tiny deviation of resonant wavelengths. Meanwhile, the mechanical properties of the mechanical resonator are measured as presented in Fig. 5. As shown in Fig. 5(a), several oscillation modes are observed within the frequency range of 1-12 MHz, including the fundamental out-of-plane (OP1) mode at $\Omega_m/2\pi = 1.82$ MHz and the fundamental in-plane (IP1) mode at $\Omega_m/2\pi = 2.88$ MHz. The inset of Fig. 5(a) shows the FEM-calculated vibration IP1 mode at 3.02 MHz, which is in good agreement with the measured one. In order to demonstrate cavity optomechanics in this system, a PSD map is developed around the IP1 vibration mode by sweeping through the $TE_{1,e}$ mode of probe cavity. By monitoring the mechanical response under the laser-cavity detuning, optical spring effect is observed. As shown in Fig. 5(b), a spring stiffening occurs in the blue-detuned regime and a spring softening occurs in the red-detuned regime, respectively. For example, in the blue-detuned regime,

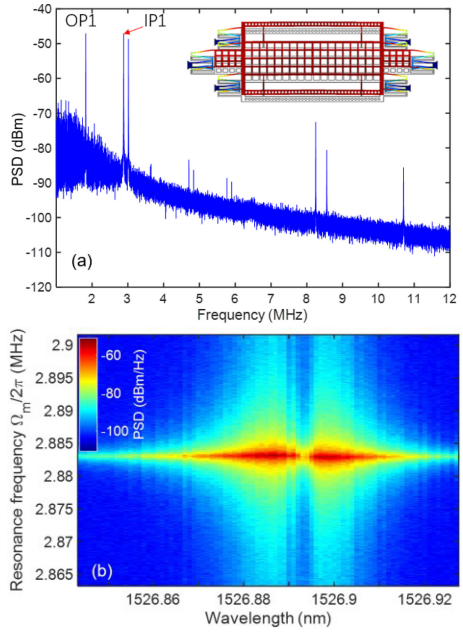


Fig. 5. Mechanical spectra of dual optomechanical cavities: (a) Mechanical spectrum of the mechanical element clamped by folded-beams. Inset is the FEM-calculated IP1 mode; (b) PSD map of mechanical resonator measured by the laser-cavity detuning.

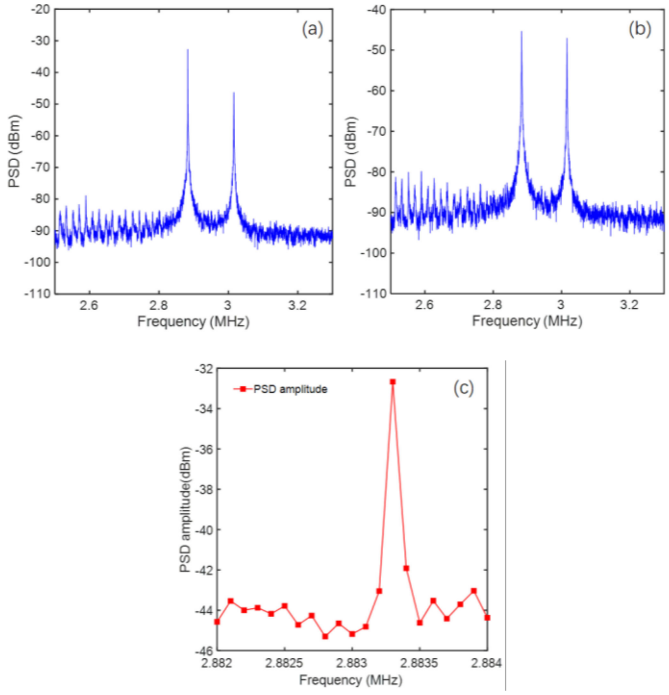


Fig. 6. Frequency response of the IP1 mode with 80 $\mu$W light input into the pump cavity: (a) RF spectrum at the on-resonance frequency; (b) RF spectrum at the off-resonance frequency; (c) Extracted amplitude of PSD spectra peaks with the frequency step of 0.1 kHz.

the mechanical resonant frequency has a slight drop first and then recovers to the initial value at the dip of the optical resonance.

In the COM system, the average static optical force in the optical cavity can be evaluated as $\mathrm{F_{opt}} = -\hbar \mathrm{g_{OM}} \mathrm{n_c} \approx 61$ pN (where, $\hbar$ is Planck constant, $\mathrm{g_{OM}}$ is optomechanical coupling strength (i.e., cavity frequency detuning vs. mechanical displacement with a unit of GHz/nm) and $\mathrm{n_c}$ is photon number circulating inside the cavity) when the light launching into the pump cavity is 80 $\mu$W. A continuous modulation signal on EOM can transform this static optical force to a dynamical one with a tuning frequency. As this dynamical optical force is acted on the optomechanical system, the behaviour of the mechanical mode of IP1 mode is dependent on this modulation frequency. Fig. 6 presents the frequency response of the PSD spectra of IP1 mode when it is characterized under the pump power of 80 $\mu$W. Note that all measurements of PSD spectra around the IP1 mode are detected from the probe cavity where the input power is 20 $\mu$W. When the modulation frequency is close to or even set at the on-resonance frequency of 2.8833 MHz as shown in Fig. 6(a), the amplitude of the resonance peak reaches up to -33 dBm which is much larger than that of the peak amplitude (-44 dBm) when the modulation is off-resonance (as indicated in Fig. 6(b)). At the on-resonance modulation frequency, a resonant oscillation between the IP1 mode motion and the driven optical force is achieved to observe a significant amplification of the amplitude of mechanical resonance peak. The frequency response of the peak amplitude of mechanical resonance is summarized in Fig. 6(c). It can be clearly seen that there is a $\sim$11 dB amplification in the mechanical resonance amplitude when the mechanical system resonantly oscillates with the driven force. As a result, it can be concluded that this modulated optical force contributes to the greatly enhanced amplification of mechanical motion in this dual optomechanical cavities system.

In order to demonstrate the effect of the optical force on the all-optical motion actuation in the COM system, an increasing light power injected into the pump cavity is conducted to observe the behaviour of the mechanical response. Here, light powers injected into the pump cavity increase from 0.08 mW to 0.75 mW, while the light launching into the probe cavity is kept as 20 $\mu$W. Under each pump power, the optical resonance should be calibrated first and the then the laser wavelength is fixed at the shoulder of the calibrated optical resonance for the motion amplification measurement. A direct comparison of the mechanical motion can be achieved through the PSD spectra readout from the probe cavity, as illustrated in Fig. 7. It can be seen that the amplitude of mechanical resonance peaks can reach a maximum to achieve harmonic oscillation when the light (or optical force) is modulated at the natural resonant frequency. However, as the light input coupled into the pump cavity is operated at the off-resonance frequency, the amplitude of the resonance peak is maintained at an average value of $-42$ dBm. Meanwhile, when the COM system turns to resonantly oscillate at the IP1 resonant frequency, the amplification of the resonance peak is increased with the optical power intensity. For example, the mechanical resonance peak amplitude can be gradually increased from the value of $-27$ dBm at the power of 0.16 mW (Fig. 7(a)) to that of $-15$ dBm at the power of 0.75 mW (Fig. 7(d)). In addition, it should be pointed out that these measured frequencies of IP1 mode under the different

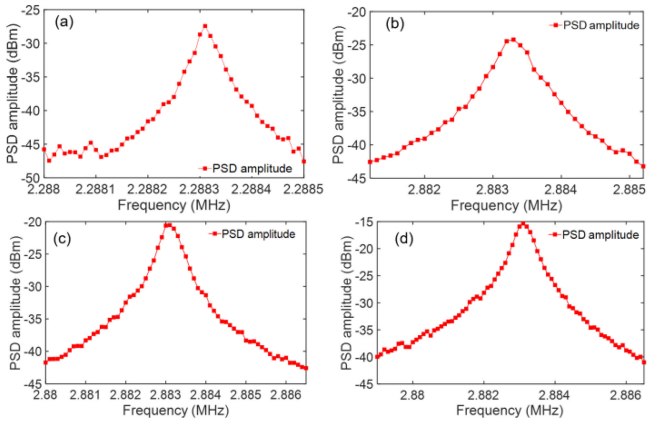


Fig. 7. Frequency response of the IP1 mode with the increasing light input power into the pump cavity: (a) 0.16 mW; (b) 0.24 mW; (c) 0.50 mW; (d) 0.75 mW.

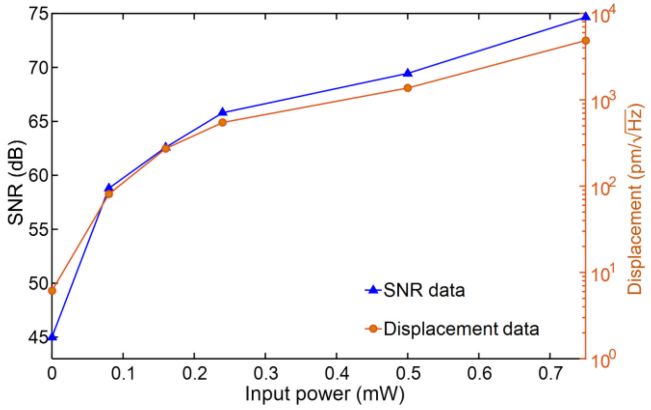


Fig. 8. Dynamical response of the IP1 mode under the increasing light input power into the pump zipper cavity.

pump powers have some tiny variation as they are modified by the dynamical backaction of the COM system. According to the theory of the optical spring effect, the mechanical resonant frequency can be changed and modulated by the laser-cavity detuning when the cavity optomechanics occurs as shown in Fig. 5(b). At the blue-detuned wavelength regime, the mechanical resonant frequency tends to be larger and the increase of the resonant frequency is proportional to the input power of pump cavities. Therefore, the measured mechanical resonant frequency of IP1 mode could have a tiny variation around 2.8833 MHz with a fluctuation of several kHz. For a better understanding of the all-optical optomechanical actuation based on the pump-probe scheme, the measured power PSD should be transduced to the displacement PSD. To obtain the corresponding displacement PSD, the relationship between the frequency-domain optical power intensity and the frequency-domain mechanical motion of the movable mechanical resonator is given as [18],

$$\mathrm{P_m}(\omega) = \frac{\mathrm{dT}}{\mathrm{d}\Delta}\frac{\mathrm{Q_o}}{\omega_c} g_{\mathrm{OM}} \mathrm{P_{det}} x(\omega) \tag{1}$$

where $\mathrm{P_{det}}$ is the off-resonance power received by the detector, and $\mathrm{dT}/\mathrm{d}\Delta$ is the optical transmission change caused by a shift of the cavity resonance frequency and it can be calculated as $\mathrm{T_d} = 0.82$ at the shoulder of the optical resonance. In this experimental system, the Newport 1811 balanced photodetector with transimpedance gain of $\mathrm{g_{ti}} = 40000$ V/W is used, and it corresponds to a photovoltaic conversion output of $\mathrm{V_m} = \mathrm{g_{ti}P_m}$. The ESA is used to obtain the power PSD of the optical signal that is modulated by the motion of the mechanical resonator in the unit of $\mathrm{V_m}^2/\mathrm{Z}$ with $\mathrm{Z} = 50\ \Omega$. Thus, the displacement PSD can be converted to power PSD intensity with dBm/Hz units by following the relation expressed as$\mathrm{PSD_{ESA}}(\omega) = 10 \cdot \log(\frac{(\mathrm{g_{ti}P_m}(\omega))^2}{\mathrm{Z}} \cdot 10^3)$. With the optomechanical coupling strength determined as 12 GHz/nm, $\mathrm{Q_o} \approx 3.0 \times 10^4$ , $\omega_c = 2\pi \times 190.47$ THz from the experimental tests, an optical displacement sensitivity of $\mathrm{P_m/x} = 6.5\ \mathrm{nW/pm}$ can be solved from Eq. (1). It indicates the measured displacement noise floor of $\sim 0.15$ fm/Hz$^{1/2}$ and a stationary motion amplitude of $\sim 61.2$ fm/Hz$^{1/2}$ for the fundamental IP1 mode at the input power of 0.08 mW. Moreover, the dynamical behaviour of the mechanical resonator under the modulated optical force is summarized in Fig. 8.

As presented in Fig. 8, it can be seen that the amplification of mechanical resonance peak is proportional to the input power into the pump cavity by solving the amplification gain as the signal-to-noise ratio (SNR) of the mechanical resonance. As the input power increases from 0.08 mW to 0.75 mW, the maximum SNR reaches up to 75 dB compared with that of stationary SNR of 45 dB (there is no light input to the pump channel). Besides, by converting the power PSD to the displacement PSD, the motion amplitude of the mechanical resonator at the right y-axis of Fig. 8 is also increased with the increasing input power when it resonantly oscillates with the frequency-tuned optical force. When the input power is 0.75 mW in the pump channel, the maximum motion amplitude is evaluated as 4.8 $\mathrm{nm}/\sqrt{\mathrm{Hz}}$. Note that this optical force can be theoretically increased by increasing the input power into the pump channel, but a saturation of the motion amplitude is observed in our measurement when the input power is larger than 0.75 mW. A possible analysis of the saturation of dynamical motion is the fact that the operating conditions of the pump and probe cavities under large mechanical motions have been greatly drifted from the shoulder of the original optical resonance. In the dual optomechanical cavity system, both the pump and probe optical cavity interact with a mutual mechanical element, so a large input power-induced dynamical motion could shift the operation points of the pump and probe cavities. Therefore, this proposed pump-probe measurement configuration is suitable for the small displacement of the mechanical resonator in which the operating point can be maintained to track the amplification of mechanical motion.

## IV. Conclusion

In this paper, an all-optical amplification of mechanical motion is experimentally demonstrated in the dual optomechanical cavities. A pump-probe configuration is proposed with two identical optical cavities and two fiber taper coupling channels. By tuning the light intensity coupled into the pump cavity, the

optical force acted on the mechanical resonator can be modulated and resonantly oscillated at the mechanical resonant frequency. With the modulation frequency swept through the mechanical resonant frequency, an amplification of mechanical resonance peak extracted from the probe channel can be observed with a large amplification gain. Besides, an increasing the optical power into the pump channel can result in the enhancement of mechanical resonance amplification. SNR of mechanical resonance peak increases from the value of 58.8 dB at the power of 0.08 mW to that of 74.7 dB at the power of 0.75 mW, which corresponds to the motion amplitude increases from 80.8 $\mathrm{pm}/\sqrt{\mathrm{Hz}}$ to 4.8 $\mathrm{nm}/\sqrt{\mathrm{Hz}}$. This all-optical amplification of mechanical motion based on the pump-probe channels paves the way for the development of optomechanical actuation. For the purpose of large-distance actuation, this optomechanical system should be optimized with the integration of a 2-DOF mechanical vibrator in the future work.

## ACKNOWLEDGMENT

The authors would like to thank professors and staffs from University of Electronics Science and Technology for their help in the device fabrication.

## REFERENCES

[1] M. Aspelmeyer, T. J. Kippenberg, and F. Marquardt, "Cavity optomechanics," *Rev. Modern Phys.*, vol. 86, 2014, Art. no. 1391.

[2] T. Liu *et al.*, "Integrated nano-optomechanical displacement sensor with ultrawide optical bandwidth," *Nature Commun.*, vol. 11, no. 1, pp. 1–7, 2020.

[3] M. Sansa *et al.*, "Optomechanical mass spectrometry," *Nature Commun.*, vol. 11, no. 1, pp. 1–7, 2020.

[4] F. Fogliano *et al.*, "Ultrasensitive nano-optomechanical force sensor operated at dilution temperatures," *Nature Commun.*, vol. 12, pp. 1–8, 2021.

[5] F. Zhou *et al.*, "Broadband thermomechanically limited sensing with an optomechanical accelerometer," *Optica*, vol. 8, pp. 350–356, 2021.

[6] B. B. Li *et al.*, "Cavity optomechanical sensing," *Nanophotonics*, vol. 10, pp. 2799–2832, 2021.

[7] H. Fu *et al.*, "Coherent optomechanical switch for motion transduction based on dynamically localized mechanical modes," *Phys. Rev. Appl.*, vol. 9, pp. 054024, 2018.

[8] J. Rosenberg, Q. Lin, and O. Painter, "Static and dynamic wavelength routing via the gradient optical force," *Nature Photon.*, vol. 3, pp. 478–483, 2009.

[9] J. T. Hill *et al.*, "Coherent optical wavelength conversion via cavity optomechanics," *Nature Commun.*, vol. 3, pp. 1–7, 2012.

[10] M. Ghadimi *et al.*, "Multichannel optomechanical switch and locking system for wavemeters," *Appl. Opt.*, vol. 59, pp. 5136–5141, 2020.

[11] A. N. Pearson *et al.*, "Radio-frequency optomechanical characterization of a silicon nitride drum," *Sci. Rep.*, vol. 10, pp. 1–7, 2020,.

[12] L. K. Chin, Y. Shi, and A.-Q. Liu, "Optical forces in silicon nanophotonics and optomechanical systems: Science and applications," *Adv. Devices Instrum.*, vol. 2020, 2020, Art. no. 1964015.

[13] G. Pan, R. Xiao, and C. Zhai, "Entanglement and output squeezing in a distant nano-electro-optomechanical system generated by optical parametric amplifiers," *Laser Phys. Lett.*, vol. 19, 2022, Art. no. 055203.

[14] H. Zheng *et al.*, "Accurate measurement of nanomechanical motion in a fiber-taper nano-optomechanical system," *Appl. Phys. Lett.*, vol. 115, no. 1, 2019, Art. no. 013104.

[15] Q. Quan, P. B. Deotare, and M. Loncar, "Photonic crystal nanobeam cavity strongly coupled to the feeding waveguide," *Appl. Phys. Lett.*, vol. 96, 2010, Art. no. 203102.

[16] F. Pan *et al.*, "Radiation-pressure-antidamping enhanced optomechanical spring sensing," *ACS Photon.*, vol. 5, pp. 4164–4169, 2018.

[17] L. Verslegers, Z. Yu, P. B. Catrysse, and S. Fan, "Temporal coupled-mode theory for resonant apertures," *J. Opt. Soc. Amer. B*, vol. 27, no. 10, pp. 1947–1956, 2010.

[18] A. G. Krause *et al.*, "A high-resolution microchip optomechanical accelerometer," *Nature Photon.*, vol. 6, pp. 768–772, 2012.